All Sciences Proceedings

5th International Conference on Applied Engineering and Natural Sciences

July 10-12, 2023 : Konya, Turkey

All Sciences Proceedings
http://as-proceeding.com/

https://www.icaens.com/

Influence of Stand-off Distance on the Blast-Resistance of Steel Plate Supported Concrete Walls

Rasid Ahmed Yildiz[1,*]

[1]*Department of Mechanical Engineering, Istanbul Technical University, Turkey*

[*]*(yildizras@itu.edu.tr)*

Abstract – The influence of stand-off distance for the protective performance and capability of the steel plate supported concrete barriers is modelled, within the current work. Steel and concrete have been used for centuries to build protective structures. Due to the military's concern with mitigating the effects of explosions and bullets, they have both collectively seen major improvements as a material for protective constructions. The significance of stand-off distance on the durability of steel plate supported concrete wall is investigated through simulations. Johnson-Cook hardening and damage molds have been used to define the mechanical behavior of steel, while concrete damage plasticity has been used to define the behavior of concrete. The growth of detonation products is modeled using the JWL equation of state, in which Comp-B is selected as explosive. Coupled-Eulerian-Lagrangian methodology is employed in the constructed finite element model. The outcomes demonstrated that the stand-off distance has a substantial impact on a structure's durability. The explosives' ability to cause damage is less effective as stand-off distance increases. For the case that the stand-off distance is 50 mm, the explosion completely destroyed both the 10 mm thick steel plate and the concrete. However, according to the simulation's findings at the stand-off distance of 300 mm, the structure has sustained relatively minor damage. Also, the steel plate functioned as a protective barrier in most cases, as designed.

Keywords – Explosion, Air Blast, JWL, CEL, Damage

I. INTRODUCTION

For ages, protective constructions have been made of concrete and steel. They both together have significantly improved as the material for defensive structures as a result of the military's interest in resisting bullet and explosion impacts. To forecast the protection of steel supported concrete structures to predict dynamic and sudden loads, several methodologies, including experimental, analytical, and computational, have been established. The numerical approach combined with some experimental verification is the most encouraging of these since it offers extensive and thorough information that can be utilized to verify and enhance engineering solutions [1–3].

Having less strength and high brittleness, conventional concrete often displays brittle failure with extremely localized damage in close-in explosions [4,5]. On contrary, advanced concretes, such as engineered cementitious composites (ECC), ultra-high-performance concrete (UHPC), etc., have been developed by the researchers over the past few decades [6] to improve the durability of concrete structures against close-in blast loads. Fiber reinforced concretes could also successfully impede the loads occurred due to the air blast loads. Next, advanced concretes displayed greater dynamic strength and a higher energy absorption ability. when compared to the concretes produced conventionally [7]. On the other hand, these high-performance concrete structures comes in with their high cost. To decrease the labor and process cost of these high performance concretes, a minimal

application has also been conducted: supportive layer of steel.

Due to the high expense of explosion experiments, numerical modeling, comprising various numerical methods and constitute equations for the concretes, is presently employed to examine the damage behavior of the structures subjected to blast loads [8,9]. The explosion resistance of structures has been studied using numerical techniques e.g. Coupled-Lagrangian-Eulerian method [10,11], smoothed-particle hydrodynamics (SPH) [12], and dynamic adaptive finite element analysis [13]. According to Wang et al. [14] An alternate tool for analyzing the blast resistance of steel supported structures to blast loads is numerical simulation. But an accurate numerical model is required to precisely represent the nonlinear dynamic response of structures to blast loads. To take into account the complicated difficulties involved, such as fluidsolid coupling, shock wave-structure interaction, damage constitutive model at high strain rate, and mesh size impacts, a comprehensive numerical model is needed.

In this work, the effect of stand-off distance on the protective behavior of concrete walls have been numerically identified. Concrete damage plasticity has been utilized to identify the behavior of concrete, Johnson-Cook hardening and damage moldes have been used to describe the mechanical behavior of the steel. Laslty, JWL equation of state is used to model the expansion of detonation products.

II. Numerical Modelling

The experimental determination of the air blast is a labor-intensive and costly process and thus performing simulations instead of experiments would decrease the costs, significantly [8]. A coupled-Lagrangian-Eulerian (CEL) mathematical representation and a finite element model were developed to compare the performance of the walls. Combining Lagrangian and Eulerian methodologies, allows the elements to move independently, bearing large deformations [15]. The commercial finite element solver Abaqus was used to execute the simulations. Dynamic-explicit analysis was selected to enable Coupled Eulerian Lagrangian approach in Abaqus.

The pressure distribution related to detonation by products is described by using Jones-Wilkins-Lee (JWL) equation of state (EOS).

The pressure distribution is given by the JWL EOS as follows [10]:

$$P = A\left(1 - \frac{w}{R_1 V}\right)e^{-R_1 V} + B\left(1 - \frac{w}{R_2 V}\right)e^{-R_2 V} + \frac{\omega E}{V} \quad (1)$$

In equation 1, P is the pressure (MPa), A and B are the linear coefficients (MPa), R_1, R_2, and ω are the nonlinear coefficients, V effective volume ratio, E is the detonation energy density (MPa-m3/m3). Comp-B is simulated as a detonator or in other words secondary explosive in the finite element simulations. The JWL EOS parameters in which the constructed FEM are tabulated in Table 1.

Table 1. JWL EOS Parameters of Comp-B

Parameter	Value
ρ_0 (g/cm^3)	1.72
D (m/s)	7980
E_0 (MPa-m^3/m^3)	8500
A (MPa)	524200
B (MPa)	7678
R_1	4.2
R_2	1.1
ω	0.34

To model the mechanical behaviour of the steel structures in the FEM, Johnson-Cook (J-C) hardening and damage models were utilized. Weldox 460E, a high strength structural steel is selected for the simulations. The J-C yield function is expressed in Eq. 2 [10]:

$$\bar{\sigma} = [\sigma_Y + K\bar{\varepsilon}^n]\left[1 + C ln\left(\frac{\dot{\bar{\varepsilon}}}{\dot{\varepsilon}_0}\right)\right]\left[1 - \left(\frac{T - T_r}{T_m - T_r}\right)^m\right] \quad (2)$$

Also, the damage function for the J-C model is represented in Eq. 3:

$$\varepsilon_f = \left[D_1 + D_2 exp\left(D_3 \frac{\sigma_m}{\bar{\sigma}}\right)\right]\left[1 + D_4 ln\left(\frac{\dot{\bar{\varepsilon}}}{\dot{\varepsilon}_0}\right)\right]\left[1 + D_5 \left(\frac{T - T_r}{T_m - T_r}\right)^m\right] \quad (3)$$

Material properties of the selected steel is given in Table 2 as follows:

Table 2. Material properties of the Weldex 460E [16]

Parameter	Value
ρ_0 (g/cm^3)	7.83
E (GPa)	205
Poisson's ratio (υ)	0.3
A (MPa)	499
B (MPa)	382
n	0.458
m	0.893
$\dot{\varepsilon_0}$ (s^{-1})	5x10^{-4}
C	0.0079
D_1	0.636
D_2	1.936
D_3	-2.969
D_4	-0.0140
D_5	1.014

Further, the material properties for the concrete is obtained from the experimental study of Hafezolghorani et al. [17] as B50 concrete. The damage plasticity material model is selected to describe the material in FEM and material and plasticity properties are tabulated in Table 3

Table 3. Material Properties of B50 Concrete [17]

Parameter	Value
Density (g/cm3)	2.44
E (GPa)	26.5
Poisson's ratio (υ)	0.2
Dilation angle	31
Eccentiricity	0.1
fb0/fc0	1.16
K	0.67
Viscosity parameter	0

Also, concrete damage plasticity (CDP) model parameters employed for the B50 concrete is listed in Table 4.

The boundary conditions of the constructed FEM is demonstrated in Fig. 1. The weight of the explosive is selected as 2 kg and the dimensions of the explosive is calculated considering its weight. Also, a concrete wall having 250 mm x 250 mm x 100 mm and a steel plate having 250 mm x 250 mm x 10 mm is designed. A quarter model has been generated for the sake of model simplicity and processor cost.

Table 4. Mechanical Behavior of B50 Concrete [17]

Compressive Stress [MPa]	**Inelastic Strain**	**Damage Parameter (C)**	**Inelastic Strain**
25.5	0	0	0
32	5.74x10^{-6}	0	5.74x10^{-6}
37.5	4.14x10^{-5}	0	4.14x10^{-5}
42	0.00010687	0	0.00010687
45.5	0.00020227	0	0.00020227
48	0.00032756	0	0.00032756
49.5	0.00048273	0	0.00048273
48	0.00066778	0	0.00066778
45.5	0.00088273	0.01	0.00088273
42	0.00112756	0.04	0.00112756
37.5	0.00140227	0.09	0.00140227
32	0.00170687	0.16	0.00170687
25.5	0.00204136	0.25	0.00204136
18	0.00240574	0.36	0.00240574
9.5	0.0028	0.49	0.0028
Tension Stress [MPa]	**Cracking Strain**	**Damage Parameter (T)**	**Cracking Strain**
5	0	0	0
0.05	0.00149432	0.99	0.00149432

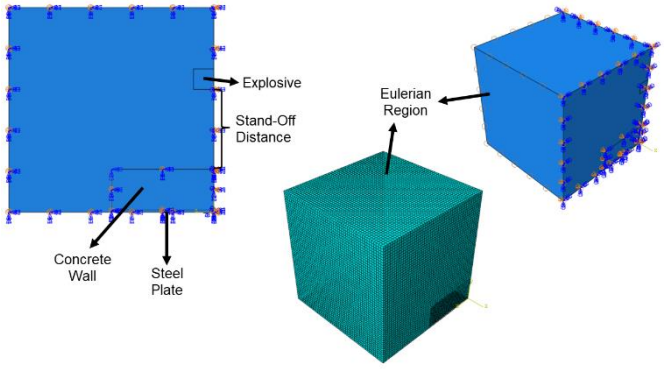

Fig. 1 Boundary Conditions of the Constructed FEM

In addition, a mesh sensitivity analysis is executed and suitable mesh sizes are selected when the convergence is under 5%.

III. Results

The simulations are carried out for different stand-off distance values including 50, 100, 200 and 300 mm. Element deletion is applied to the elements that

lost their load-carrying capacity. Fig.2 shows the steps of the expansion of detonation products in FEM. It should be noted that the stand-off distance is set to 50 mm in the FEM that is represented in Fig.2.

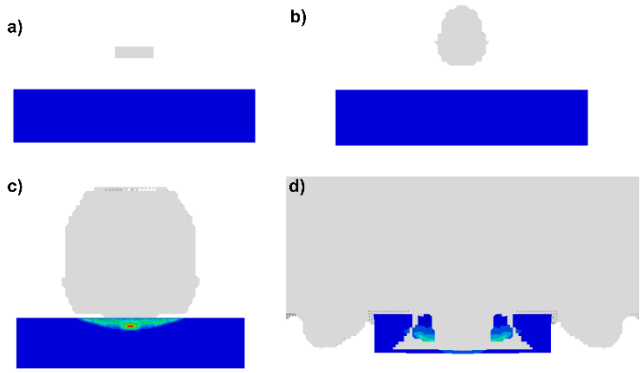

Fig. 2 Expansion of Detonation Prodcuts a) Step Time=0 b) Step Time=10 μs c) Step Time= 20 μs d) Step Time= 50 μs

Fig.3 demonstrates the final shape of the steel supported structure when the stand-off distance is 50 mm. It is clear that the explosion resulted a complete damage on both concrete and also the 10 mm thick steel plate. On one side, the level of equivalent stress did not exceed 800 MPa due to deletion of elements that lost their load-carrying capacity. Bending of the steel is also observed due to the propagation of the shock waves.

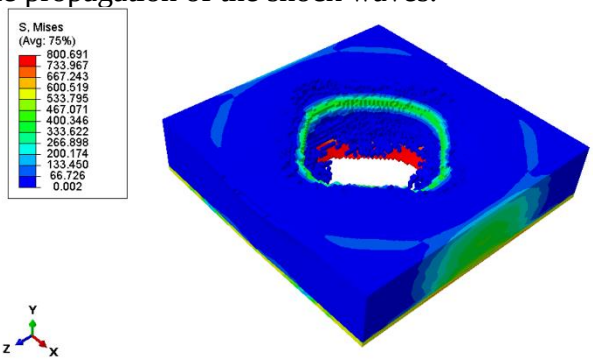

Fig. 3 The final shape of the steel supported structure when the stand-off distance is 50 mm.

Moreover, Fig. 4 represents the final demonstration of the steel supported structure when the stand-off distance is 100 mm. Both the concrete and steel is penetrated via expansion of detonation products. Similar to the 50 mm stand-off distance result, bending is observed on the structure.

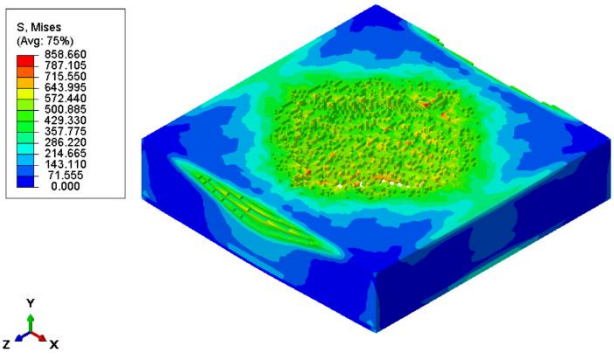

Fig. 4 The final shape of the steel supported structure when the stand-off distance is 100 mm.

Next, Fig. 5 exhibits the final step of the simulation executed when the stand-off distance is set to 200 mm. In this scenario, damage is observed in the concrete but could not penetrate the steel. The protective ability of the steel supported structure can be seen. In addition, the level of stress values remained under 700 MPa, roughly.

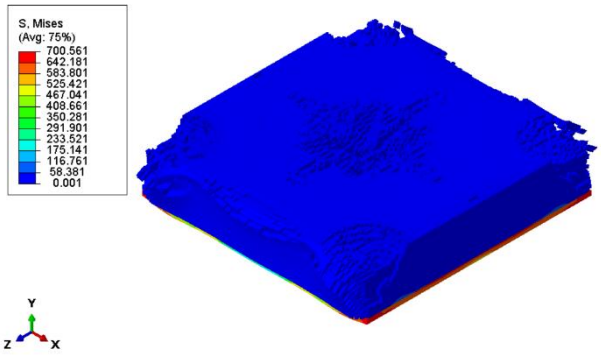

Fig. 5 The final shape of the steel supported structure when the stand-off distance is 200 mm.

Lastly, the simulation results for the stand-off distance of 300 mm can be seen in Fig. 6. In this case, a relatively minor damage has been observed on the concrete. The steel plate represented a plastic deformation without having any damage or failure.

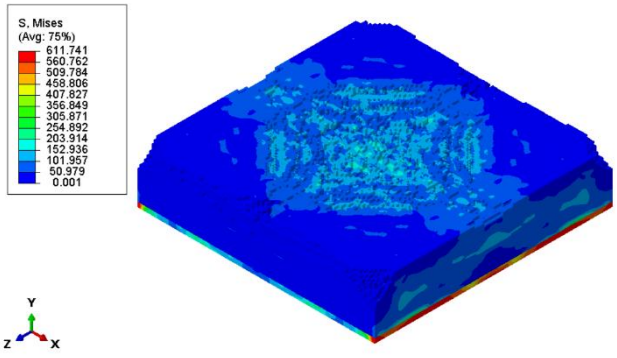

Fig. 6 The final shape of the steel supported structure when the stand-off distance is 300 mm.

Further, the time after the ignigition started for the explosive, Mises equivalent stress on the steel plate is plotted in Fig. 7 for the selected elements on the steel plate. According to the Fig. 7 the increasing stand-off distance delayed the time for the stress occurred on the structure, as a result of shock wave propagation, as expected. Also, the equivalent stress levels shows a decrease when the stand-off distance increased. This tendencany is also apparent in the final shapes shown in Fig. 3 to Fig. 6.

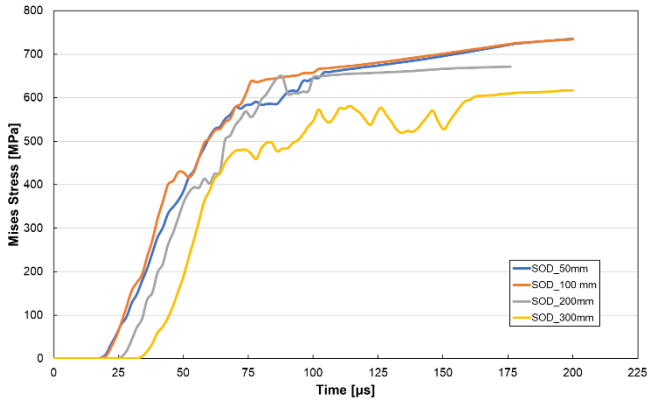

Fig. 7 Equivalent stress on the steel plate regarding time.

IV. DISCUSSION

This should explore the significance of the results of the work, not repeat them.

It is obvious that the explosion completely destroyed the 10 mm thick steel plate and the concrete. The spread of the shock waves causes the steel to bend, which is also shown. Also, the shock waves generates larger stress values when compared with the increasing values of stand-off distance.

On the contrary, when the explosive is aligned to a distance of 300 mm on the concrete, in this instance, a small amount of concrete damage has been seen. The steel plate showed a plastic deformation but had no breaks or damage.

This behaviour is also can be seen when the equilavent strain changes over time is further researched in Fig. 8.

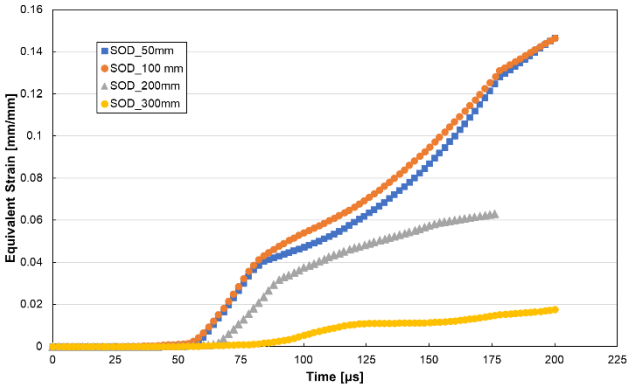

Fig. 8 Equivalent strain on the steel plate regarding time.

Equivalent strain on the steel plate is well-agree with the damage behaviour of the structure which are shown in Fig. 3 to Fig. 6. The results for the stand off distance of 50 mm and 100 mm are similar. On the contrary, increasing the stand-off distance to 300 mm rather slows down both the speed of plastic deformation and the level of plastic deformation.

V. CONCLUSION

Within the current work, the effect of stand-off distance on the blast resistance of steel plate supported concrete walls have been investigated, numerically. The results showed that the stand-off distance significantly affects the resistance of structures. Increasing stand-off distance reduces the damage ability of the explosives. Although, the explosion process is completed within microseconds, a significant delay is observed for the increasing stand-off distances that shock waves to reach the structure. Also, a jetting effect for the explosive can be seen for the low stand-off distance simulations, which enhance the destruction capability of the explosive. Thus, to reduce the damage in the structures having a possibility of closer explosions, a thicker steel plate could be used. Also, it can be concluded that the protective effect of steel plate is apparent in most cases.

REFERENCES

[1] Islam, M.J., Swaddiwudhipong, S., Liu, Z.S., (2012). Penetration of concrete targets using a modified Holmquist-Johnson-Cook material model. International Journal of Computational Methods. 9(4). doi: 10.1142/S0219876212500569.

[2] Huang, R., Hu, L., Qin, J., Jiang, D., Meng, L., (2021). Effect of Free Water on the Mechanical Properties and Blast Resistance of Concrete. KSCE Journal of Civil Engineering. 25(8): 3084–96. doi: 10.1007/s12205-021-2169-0.

[3] Yildiz, R.A., (2021). Investigation of the explosive type on the high strain forming of OFHC copper tube.

Journal of Strain Analysis for Engineering Design. doi: 10.1177/03093247211021240.

[4] Shu, Y., Wang, G., Lu, W., Chen, M., Lv, L., Chen, Y., (2022). Damage characteristics and failure modes of concrete gravity dams subjected to penetration and explosion. Engineering Failure Analysis. 134(January): 106030. doi: 10.1016/j.engfailanal.2022.106030.

[5] Li, J., Wu, C., Hao, H., (2015). Investigation of ultra-high performance concrete slab and normal strength concrete slab under contact explosion. Engineering Structures. 102: 395–408. doi: 10.1016/j.engstruct.2015.08.032.

[6] Li, J., Wu, C., Hao, H., (2015). An experimental and numerical study of reinforced ultra-high performance concrete slabs under blast loads. Materials and Design. 82: 64–76. doi: 10.1016/j.matdes.2015.05.045.

[7] Liu, C., Liu, J., Wei, J., Xu, S., Su, Y., (2022). Parametric Study on Contact Explosion Resistance of Steel Wire Mesh Reinforced Geopolymer Based Ultra-High Performance Concrete Slabs Using Calibrated Continuous Surface Cap Model. Buildings. 12(11). doi: 10.3390/buildings12112010.

[8] Yildiz, R.A., (2022). Explosive Forming of Precipitation-Hardened Aluminum Alloy Tubes. Combustion, Explosion and Shock Waves. 58(6): 738–50. doi: 10.1134/S0010508222060119.

[9] Das, N., Nanthagopalan, P., (2022). State-of-the-art review on ultra high performance concrete - Ballistic and blast perspective. Cement and Concrete Composites. 127(December 2021): 104383. doi: 10.1016/j.cemconcomp.2021.104383.

[10] Yildiz, R.A., (2023). A numerical investigation on the effect of transfer medium in explosive forming. International Journal of Advanced Manufacturing Technology.: 3249–65. doi: 10.1007/s00170-023-11323-2.

[11] Wang, G., Zhang, S., (2014). Damage prediction of concrete gravity dams subjected to underwater explosion shock loading. Engineering Failure Analysis. 39: 72–91. doi: 10.1016/j.engfailanal.2014.01.018.

[12] Yang, G., Wang, G., Lu, W., Yan, P., Chen, M., Wu, X., (2018). A SPH-Lagrangian-Eulerian Approach for the Simulation of Concrete Gravity Dams under Combined Effects of Penetration and Explosion. KSCE Journal of Civil Engineering. 22(8): 3085–101. doi: 10.1007/s12205-017-0610-1.

[13] Emamzadeh, S.S., Ahmadi, M.T., Mohammadi, S., Biglarkhani, M., (2015). Dynamic adaptive finite element analysis of acoustic wave propagation due to underwater explosion for fluid-structure interaction problems. Journal of Marine Science and Application. 14(3): 302–15. doi: 10.1007/s11804-015-1322-x.

[14] Wang, G., Lu, W., Yang, G., Yan, P., Chen, M., Zhao, X., et al., (2020). A state-of-the-art review on blast resistance and protection of high dams to blast loads. International Journal of Impact Engineering. 139(July 2019). doi: 10.1016/j.ijimpeng.2020.103529.

[15] Tetik, T., Yildiz, R.A., Labanieh, A.R., Yoruk, B., Kursun Bahadir, S., Kalaoglu, F., et al., (2021). Hydrodynamic modeling of e-textile fabric washing behavior by the Coupled Eulerian–Lagrangian method. Textile Research Journal. 91(9–10): 1117–31. doi: 10.1177/0040517520973455.

[16] Dey, S., Børvik, T., Hopperstad, O.S., Langseth, M., (2006). On the influence of fracture criterion in projectile impact of steel plates. Computational Materials Science. 38(1): 176–91. doi: 10.1016/j.commatsci.2006.02.003.

[17] Hafezolghorani, M., Hejazi, F., Vaghei, R., Jaafar, M.S. Bin., Karimzade, K., (2017). Simplified damage plasticity model for concrete. Structural Engineering International. 27(1): 68–78. doi: 10.2749/101686616X1081.